evaporated to dryness under a nitrogen stream at 30°C. The residues were dissolved in 100 μL of mobile phase, and a 50-μL portion of the sample was subjected to HPLC. HPLC analyses were performed using an L-7100 pump (Hitachi, Tokyo, Japan), an L-7400 UV detector (Hitachi), an L-7200 autosampler (Hitachi), an L-7500 integrator (Hitachi), and an 865-CO column oven (Jasco, Tokyo, Japan). The flow rate was 1.0 mL/min, and the column temperature was 35°C. The eluent was monitored at 227 nm with a base line adjuster Uni-3 (Union, Gunma, Japan). The analytical column was a Mightysil (4.6 × 150 mm; 5 μm) column (Kanto Chemical, Tokyo, Japan), and the mobile phase was acetonitrile:0.02 M ammonium acetate buffer (pH 5.0) = 4:6. Aliquots of aqueous solutions of paclitaxel, 6α-hydroxypaclitaxel, and 3′-*p*-hydroxypaclitaxel were added to blank plasma samples from healthy subjects to make calibration curves. The quantification of paclitaxel, 6α-hydroxypaclitaxel, and 3′-*p*-hydroxypaclitaxel was performed by comparing the HPLC peak heights to those of authentic standards with reference to an internal standard. The limits of quantification of paclitaxel, 6α-hydroxypaclitaxel, and 3′-*p*-hydroxypaclitaxel were 15 nM, 5 nM, and 1 nM, respectively. The intraday and interday precision and accuracy were confirmed to be <10%.

Pharmacokinetic Analysis

Pharmacokinetic parameters of paclitaxel and its metabolites were calculated by a moment analysis (MULTI). The areas under the plasma concentrations time curve (AUC) were obtained using the trapezoidal rule and extrapolation to infinity by linear regression. The total plasma clearance of paclitaxel was calculated by dividing the dose by the AUC.

Genotyping of *CYP2C8*, *CYP3A4*, and *MDR1* Alleles

Genomic DNA was extracted from peripheral lymphocytes using the Puregene DNA isolation kit. *CYP2C8*2* (I269F), *CYP2C8*3* (R139K, K399R), *CYP2C8*4* (I264M), and *CYP2C8*5* (frameshift) alleles and the single nucleotide polymorphisms (SNPs) leading to T130N, E154D, N193K, K249R, L390S, P404A, and H411L were genotyped by polymerase chain reaction–restriction fragment length polymorphism (PCR-RFLP) or allele-specific PCR methods established in our laboratory.[16] *CYP3A4*4* (I118V), *CYP3A4*5* (P218R), *CYP3A4*6* (frameshift), and *CYP3A4*16* (T185S) alleles were genotyped as described previously.[17,18] *CYP3A4*17* (F189S) allele was genotyped by allele-specific PCR method established in the present study as follows: genomic DNA samples (50-100 ng) were added to the PCR mixtures (25 μl) consisting of 1 × PCR buffer (67 mM Tris-HCl buffer [pH 8.8], 16.6 mM $[NH_4]_2SO_4$, 0.45% Triton X-100, 0.02% gelatin), 1.5 mM $MgCl_2$, 0.4 μM primers, 250 μM dNTPs, and 1 U of Taq DNA polymerase. Used primers were *17S (5′-ATGGAGTGTGATAGAAG-3′) and *17AS-wt (5′-GTCGATGTTCACTCCAA-3′) or *17AS-mt (5′-GTCGATGTTCACTCCAG-3′). After an initial denaturation at 94°C for 3 minutes, the amplification was performed by denaturation at 94°C for 30 seconds, annealing at 53°C for 30 seconds, and extension at 72°C for 20 seconds for 30 cycles. The final extension step was performed at 72°C for 5 minutes. The expected size of the PCR product was 210 bp. Genetic polymorphisms of C1236T in exon 12 (synonymous), G2677T/A in exon 21 (Ala893Ser/Thr), and C3435T in exon 26 (synonymous) in *MDR1* gene were determined by methods reported previously.[19,20] In all PCR-RFLP analyses except *CYP3A4*5*, restriction enzymes digest the wild-type PCR product on at least 1 site. In the mutated PCR product, a recognition site of the restriction enzyme disappears owing to the mutation. It was confirmed that the PCR products were almost completely digested if these were wild type. In the PCR-RFLP method for *CYP3A4*5*, in which the mutated PCR product is digested by *Cla* I, we confirmed that the restriction enzyme exactly worked using another PCR product containing the recognition site as a positive control. In AS-PCR analyses, positive controls of wild type and mutant type were made by PCR using wild-specific primer and mutant-specific primer, respectively, with the PCR condition at low anneal temperature. With these controls, we confirmed that the wild-specific primer and mutant-specific primer could specifically anneal to the wild type and mutant type, respectively.

Analysis of Adverse Effects

Adverse reactions were assessed using the data from all courses of chemotherapy in each patient (a total of 116 courses in 23 patients). As indicators of myelosuppression, leukocytes, neutrophils, and platelets were counted every 3 days after drug administration. The nadirs of the counts were used as reflections of the maximal myelosuppression. The other adverse

reactions analyzed were gastrointestinal toxicity and hepatotoxicity. As indicators of hepatotoxicity, aspartate aminotransferase (AST) and alanine aminotransferase (ALT) were measured every week after the treatment. These toxicities were assessed based on common toxicity criteria (CTC) grading (National Cancer Institute). The highest grades observed throughout all courses were assessed. Since the assessment of the extent of arthralgia, myalgia, and neurotoxicity is rather difficult, these parameters were excluded from the analysis.

Statistical Analyses

Fisher's exact test was used to verify agreement of the observed genotype frequencies with those expected ones (Hardy-Weinberg equilibrium). Pharmacokinetic data are presented as mean ± SD. The relationships between the pharmacokinetic parameters and *MDR1* alleles or CTC grading were investigated by Kruskal-Wallis test or Mann-Whitney *U* test using an InStat computer program (GraphPad Software, San Diego, Calif). $P < .05$ was considered statistically significant.

RESULTS

Pharmacokinetics of Paclitaxel in Ovarian Cancer Patients

The plasma concentrations of paclitaxel and its metabolites were simultaneously measured by HPLC. As shown in Figure 1, none of these chromatograms showed any interfering peaks. The concentrations of paclitaxel and its metabolites increased throughout the infusion of paclitaxel and peaked at the end of infusion, followed by a rapid decrease after completion of administration (Figure 2). The pharmacokinetic parameters of paclitaxel and its metabolites are summarized in Table I. The AUC of paclitaxel ranged from 11 845 to 35 096 nM•h. The interindividual difference in the clearance of paclitaxel was approximately 3-fold (9.3-26.7 L/h) in 23 patients. The AUC values of 6α-hydroxypaclitaxel (185-3077 nM•h) and 3′-*p*-hydroxypaclitaxel (37-423 nM•h) were lower compared with the AUC of paclitaxel. However, the interindividual differences in the AUC values of 6α-hydroxypaclitaxel (17-fold) and 3′-*p*-hydroxypaclitaxel (11-fold) were relatively large. The AUC ratios of paclitaxel/6α-hydroxypaclitaxel and paclitaxel/3′-*p*-hydroxypaclitaxel calculated as the metabolic index of CYP2C8 and CYP3A4 showed large interindividual variability (13- and 12-fold, respectively). Liquid chromatography-tandem mass spec-

Table I Pharmacokinetic Parameters of Paclitaxel and Its Metabolites (n = 23)

Parameter	Mean ± SD	Range
Paclitaxel		
CL, L/h	16.7 ± 4.9	9.3-26.7
AUC, nM•h	20 839 ± 6300	11 845-35 096
6α-hydroxypaclitaxel		
AUC, nM•h	857 ± 718	185-3077
3′-*p*-hydroxypaclitaxel		
AUC, nM•h	221 ± 115	37-423
AUC ratio		
Paclitaxel/ 6α-hydroxypaclitaxel	38.9 ± 22.3	7.5-97.1
Paclitaxel/ 3′-*p*-hydroxypaclitaxel	128.1 ± 98.7	41.9-510.0

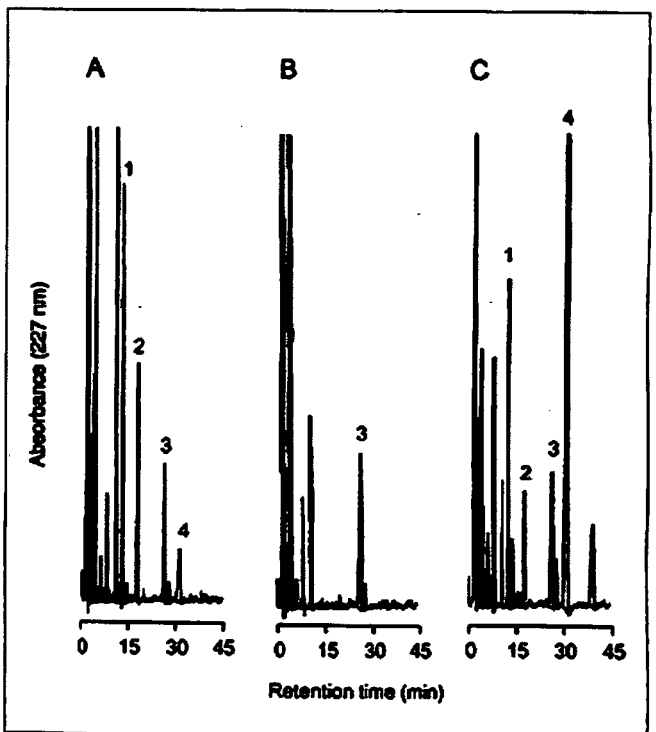

Figure 1. Representative chromatograms of paclitaxel and its metabolites. Analysis of paclitaxel, 6α-hydroxypaclitaxel, and 3′-p-hydroxypaclitaxel from plasma spiked with authentic standards (A). Plasma sample before (B) and after (C) infusion of paclitaxel. Peaks: 1, 3′-p-hydroxypaclitaxel (12.7 minutes); 2, 6α-hydroxypaclitaxel (17.8 minutes); 3, docetaxel as an internal standard (26.5 minutes); 4, paclitaxel (31.5 minutes).

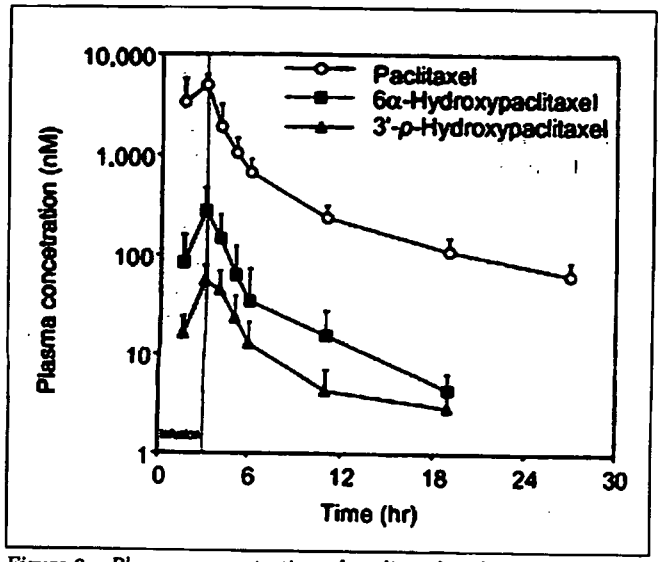

Figure 2. Plasma concentration of paclitaxel and its metabolites in ovarian cancer patients after a 3-hour infusion of paclitaxel. Each point represents the mean ± SD (n = 23).

trometry analyses showed that the plasma concentration of 6α,3′-*p*-dihydroxypaclitaxel was prominently lower than those of 6α-hydroxypaclitaxel and 3′-*p*-hydroxypaclitaxel (data not shown).

Genotypinges of *CYP2C8*, *CYP3A4*, and *MDR1* Genes

No patient had any *CYP2C8* variant for the 11 SNPs examined. Two subjects were heterozygous for the *CYP3A4*16* allele (Table II). The other SNPs of the *CYP3A4* gene were not found in the patients in the present study. There was no relationship between the *CYP3A4*16* allele and the pharmacokinetic parameters of paclitaxel and its metabolites. As for the *MDR1* gene, 1 patient was heterozygous for –129C and homozygous for 1236C simultaneously and 2 patients were heterozygous for 1236C (Table II). For the SNP of G2677T/A, 1 patient had G/G, 11 had G/T, 2 had G/A, 6 had T/T, and 3 had T/A. For the SNP of C3435T, 5 patients had C/C, 12 had C/T, and 6 had T/T. Thus, the fre-

Table II Genotype of *CYP3A4* and *MDR1* Genes in Each Patient

Patient	*CYP3A4*16*	*MDR1*			
		T-129C	T1236C	G2677T/A	C3435T
1	C/G	T/T	T/T	G/G	C/C
2	C/G	T/T	T/T	G/T	C/C
3	C/C	T/T	T/T	G/T	C/C
4	C/C	T/T	T/T	G/A	C/C
5	C/C	T/C	C/C	G/A	C/C
6	C/C	T/T	T/T	G/T	C/T
7	C/C	T/T	T/T	G/T	C/T
8	C/C	T/T	T/T	G/T	C/T
9	C/C	T/T	T/T	G/T	C/T
10	C/C	T/T	T/T	G/T	C/T
11	C/C	T/T	T/T	G/T	C/T
12	C/C	T/T	T/T	G/T	C/T
13	C/C	T/T	T/T	G/T	C/T
14	C/C	T/T	T/T	T/A	C/T
15	C/C	T/T	T/T	T/A	C/T
16	C/C	T/T	T/C	T/A	C/T
17	C/C	T/T	T/T	T/T	C/T
18	C/C	T/T	T/T	T/T	T/T
19	C/C	T/T	T/T	T/T	T/T
20	C/C	T/T	T/T	T/T	T/T
21	C/C	T/T	T/T	T/T	T/T
22	C/C	T/T	T/T	T/T	T/T
23	C/C	T/T	T/C	G/T	T/T

Shading indicates nucleotides in mutant type.

quencies of –129C, 1236C, 2677T, 2677A, and 3435T alleles in the 23 Japanese patients were 2.2%, 8.7%, 56.5%, 4.4%, and 52.2%, respectively. The genotype frequencies were in the Hardy-Weinberg equilibrium (P values were higher than .58). The pharmacokinetic parameters of paclitaxel and 6α-hydroxypaclitaxel were not significantly different among the groups with different genotypes of *MDR1* gene (Figure 3). Notably, subjects possessing the 3435T allele had a significantly ($P < .05$) higher AUC of 3′-*p*-hydroxypaclitaxel compared with those possessing the 3435C allele. Although it has been reported that the SNPs of C3435T and G2677T/A are closely linked,[19,21] the present study did not demonstrate any significant differences between the pharmacokinetic parameters of paclitaxel or its metabolites and the haplotypes (data not shown).

Adverse Effects

The analyzed toxicities were myelosuppression, gastrointestinal toxicity, and hepatotoxicity. None of the 23 patients experienced severe hypersensitivity reactions leading to discontinuation of the paclitaxel administration. Leukocytopenia and thrombocytopenia of grade 3 were observed in 17 patients and 5 patients, respectively. Gastrointestinal toxicity of grade 3, as evidenced by severe nausea and vomiting, was observed in 7 patients. Severe hepatotoxicity was not observed in any patients. Figure 4 shows scatterplots of the toxicity grade versus the AUC of paclitaxel. Statistical analyses revealed that only leukocytopenia was significantly ($P < .05$) related to the AUC of paclitaxel. No relationship was observed between the toxicities and the AUC values of the metabolites (data not shown).

DISCUSSION

Paclitaxel is mainly metabolized to 6α-hydroxypaclitaxel by CYP2C8 and, to a minor extent, to 3′-*p*-hydroxypaclitaxel by CYP3A4. Among several alleles of *CYP2C8*, in vitro studies demonstrated that the *CYP2C8*2*, *CYP2C8*3*, and *CYP2C8*4* alleles and the P404A variant showed decreased paclitaxel 6α-hydroxylase activity.[22-24] The *CYP2C8*5* allele is expected to lack enzymatic activity owing to an early stop codon.[25] Concerning *CYP3A4* genetic polymorphisms, *CYP3A4*4*, *CYP3A4*5*, *CYP3A4*6*, *CYP3A4*16*, and *CYP3A4*17* are associated with decreased enzymatic activity.[17,26,27] However, no information is available concerning the effects of polymorphisms of these genes on the pharma-cokinetics of paclitaxel. This is the first study to investigate such correlations in ovarian cancer patients. In our protocol, carboplatin was administered 30 minutes after the infusion of paclitaxel. However, no pharmacokinetic interactions have been reported between paclitaxel and carboplatin at standard doses.[28-30] The AUC of paclitaxel varied within a relatively narrow range (~3-fold). When

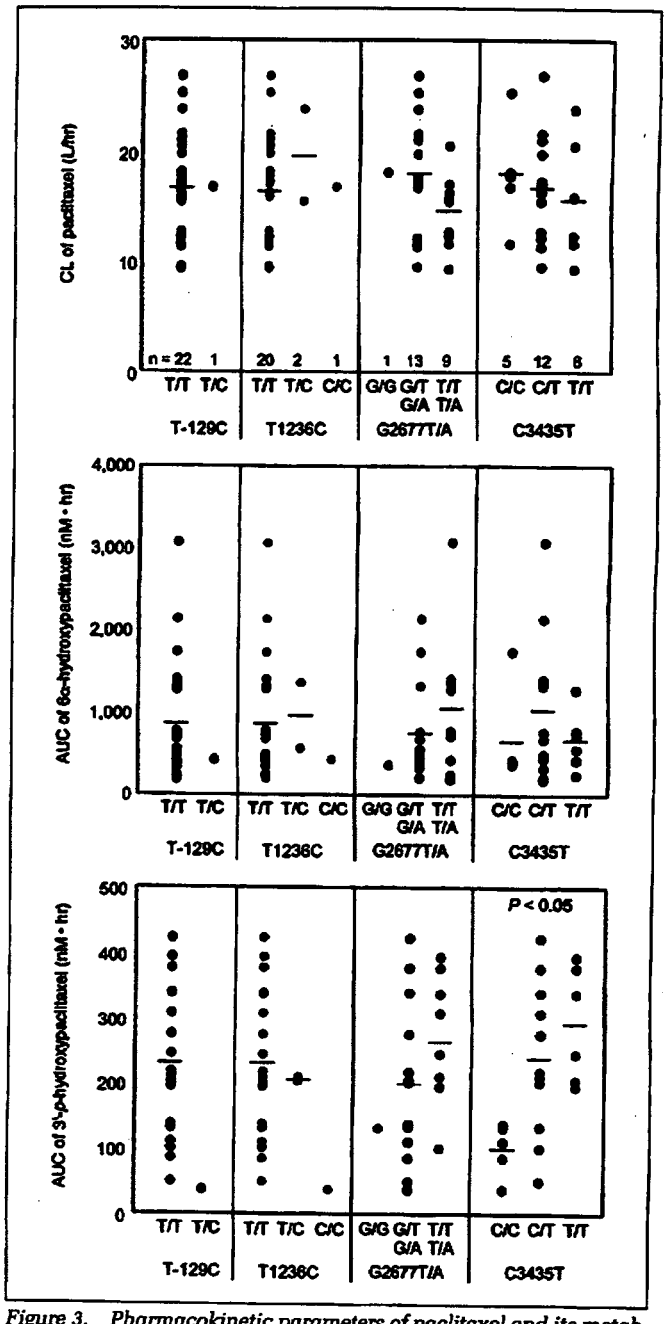

Figure 3. Pharmacokinetic parameters of paclitaxel and its metabolites in ovarian cancer patients with different genotypes for the MDR1 *gene. Each point represents an individual (n = 23), and the mean value in each genotype is shown as the bar.*

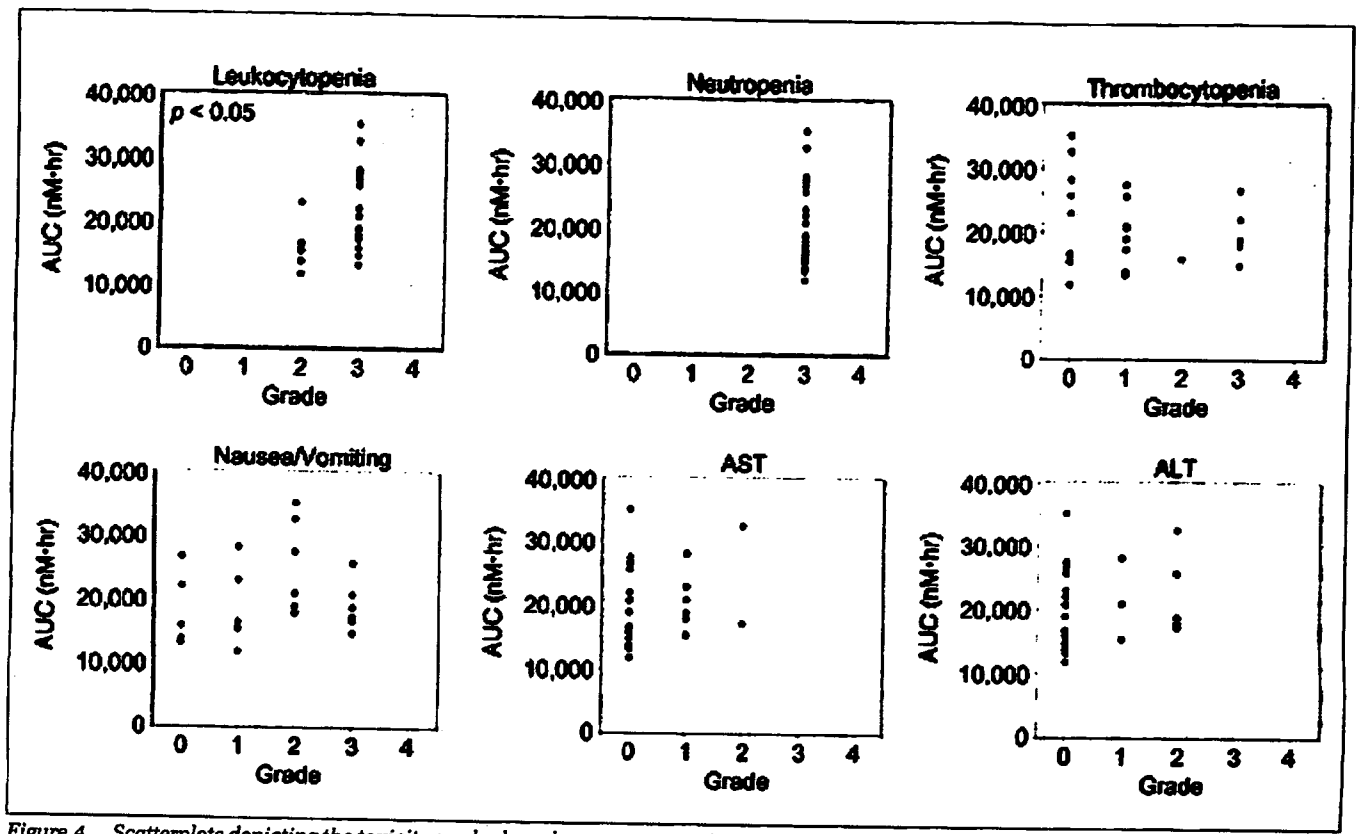

Figure 4. Scatterplots depicting the toxicity grades based on common toxicity criteria grading versus the AUC of paclitaxel. Each point represents an individual (n = 23).

myelosuppression and gastrointestinal toxicity are evaluated in patients, it should be minded that we cannot interpret whether such toxicities are by paclitaxel or carboplatin. However, among various adverse effects, only severe leukocytopenia was significantly related to the AUC of paclitaxel, confirming that the AUC of this drug is a critical parameter of myelosuppression.

In the genotyping analyses, no *CYP2C8* variants were found for 11 SNPs examined in the 23 ovarian cancer patients. The sample number would be too small to investigate the relationship between the genetic polymorphism of *CYP2C8* and pharmacokinetics and/or pharmacodynamics of paclitaxel. Our concurrent study of *CYP2C8* genotyping in 360 Japanese healthy subjects[16] revealed that the variant alleles are very rare in Japanese since only the *CYP2C8*5* allele was found with allele frequency of 0.25%. Therefore, we might not be able to find relevance between the *CYP2C8* genotype and pharmacokinetics/pharmacodynamics of paclitaxel even if several hundreds of patients were studied. Genotyping of the gene might therefore have limited utility in predicting adverse effects from paclitaxel in Japanese cancer patients. In contrast, these variant alleles are more frequent (2%-15%) in Caucasians and African Americans.[22,23] Studies in these populations will provide more critical information on the effects of SNPs on the pharmacokinetics of paclitaxel.

Large interindividual variations were observed in the AUC ratios of paclitaxel/6α-hydroxypaclitaxel and paclitaxel/3′-*p*-hydroxypaclitaxel calculated as metabolic indices of CYP2C8 and CYP3A4, respectively. The variability might be due to differences in the expression levels of these enzymes and/or functional polymorphisms that have not been identified. However, since the interindividual difference in the AUC or clearance of paclitaxel was at most 3-fold, such interindividual differences (>10-fold) in the metabolic potency for paclitaxel assessed by the metabolic indices might not be important for the efficacy and toxicity of paclitaxel.

A major part of paclitaxel is excreted to feces as the parent drug and its metabolites.[31] Gianni et al[32] reported that measurable metabolite concentrations represent an overflow in situations of relative saturation or

blockade of biliary elimination. P-glycoprotein is an important factor in the biliary excretion of many drugs, and the involved process often exhibits considerable interindividual variability that may be genetically determined. Paclitaxel is also a substrate of P-glycoprotein.[9-12] Therefore, we focused on the relationship between the pharmacokinetic parameters of paclitaxel and the genetic polymorphism of the *MDR1* gene. A number of SNPs have been identified in the human *MDR1* gene.[19,21,33,34] Of these SNPs, T-129C (noncoding), T1236C (Gly412Gly, wobble), G2677T/A (Ala893Ser/Thr), and C3435T (Ile1145Ile, wobble) are associated with alterations in the expression of P-glycoprotein and pharmacokinetic profiles of certain clinically used drugs.[19,21,34] The present study showed an apparent association between the presence of 3435T allele and increased AUC of 3′-*p*-hydroxypaclitaxel. This result may indicate that 3′-*p*-hydroxypaclitaxel is also a substrate of P-glycoprotein with higher affinity than paclitaxel itself, although there is no in vitro data to support this at present. This appears to be the first in vivo observation that the allelic variant of *MDR1* may functionally affect the pharmacokinetics of a metabolite of paclitaxel.

In conclusion, this study demonstrated that there are relatively small individual differences in the pharmacokinetics of paclitaxel among Japanese ovarian cancer patients. Genetic polymorphisms of *CYP2C8*, *CYP3A4*, and *MDR1* genes might not be essential to predict adverse effects of paclitaxel. This information would be valuable for physicians engaged in the treatment of ovarian cancers.

We acknowledge Mr Brent Bell for reviewing the manuscript.

REFERENCES

1. Horwitz SB, Lothstein L, Manfredi JJ, et al. Taxol: mechanisms of action and resistance. *Ann N Y Acad Sci.* 1986;466:433-444.

2. Monsarrat B, Alvinerie P, Wright M, et al. Hepatic metabolism and biliary excretion of Taxol in rats and humans. *J Natl Cancer Inst Monogr.* 1993;15:39-46.

3. Rahman A, Korzekwa KR, Grogan J, Gonzalez FJ, Harris JW. Selective biotransformation of Taxol to 6α-hydroxytaxol by human cytochrome P450 2C8. *Cancer Res.* 1994;54:5543-5546.

4. Harris JW, Katki A, Anderson LW, Chmurny GN, Paukstelis JV, Collins JM. Isolation, structural determination, and biological activity of 6 alpha-hydroxytaxol, the principal human metabolite of Taxol. *J Med Chem.* 1994;37:706-709.

5. Sparreboom A, Huizing MT, Boesen JJB, Nooijen WJ, van Tellingen O, Beijnen JH. Isolation, purification and biological activity of mono- and dihydroxylated paclitaxel (Taxol) metabolites from human faeces. *Cancer Chemother Pharmacol.* 1995;36:299-304.

6. Kumar G, Ray S, Walle T, et al. Comparative in vitro cytotoxic effects of Taxol and its major human metabolite 6α-hydroxytaxol. *Cancer Chemother Pharmacol.* 1995;36:129-135.

7. Harris JW, Kim BR, Guengerich FP, Collins JM. Metabolism of Taxol by human hepatic microsomes and liver slices: participation of cytochrome p450 3A4 and an unknown P450 enzyme. *Cancer Res.* 1994;54:4026-4035.

8. Cresteil T, Monsarrat B, Alvinerie P, Treluyer JM, Vieira I, Wright M. Taxol metabolism by human liver microsomes: identification of cytochrome P450 isozymes involved in its biotransformation. *Cancer Res.* 1994;54:386-392.

9. Sparreboom A, van Asperen J, Mayer U, et al. Limited oral bioavailability and active epithelial excretion of paclitaxel (Taxol) caused by P-glycoprotein in the intestine. *Proc Natl Acad Sci U S A.* 1997;94:2031-2035.

10. van Asperen J, van Tellingen O, Sparreboom A, et al. Enhanced oral bioavailability of paclitaxel in mice treated with the P-glycoprotein blocker SDZ PSC 833. *Br J Cancer.* 1997;76:1181-1183.

11. Wu H, Hait WN, Yang J-M. Small interfering RNA-induced suppression of MDR1 (P-glycoprotein) restores sensitivity to multidrug-resistant cancer cells. *Cancer Res.* 2003;63:1515-1519.

12. Penson RT, Oliva E, Skates SJ, et al. Expression of multidrug resistance-1 protein inversely correlates with paclitaxel response and survival in ovarian cancer patients: a study in serial samples. *Gynecol Oncol.* 2004;93:98-106.

13. Daly AK. Pharmacogenetics. In: Woolf TF, ed. *Handbook of Drug Metabolism.* New York, NY: Marcel Dekker; 1999:175-202.

14. Schwab M, Eichelbaum M, Fromm MF. Genetic polymorphisms of the human MDR1 drug transporter. *Annu Rev Pharmacol Toxicol.* 2003;43:285-307.

15. Willey TA, Bekos EJ, Gaver RC, Dunca GF, Tay LK. High-performance liquid chromatographic procedure for the quantitative determination of paclitaxel (Taxol®) in human plasma. *J Chromatogr.* 1993;621:231-238.

16. Nakajima M, Fujiki Y, Noda K, et al. Genetic polymorphisms of *CYP2C8* in Japanese population. *Drug Metab Dispos.* 2003;31:687-690.

17. Hsieh KP, Lin YY, Cheng CL, et al. Novel mutations of CYP3A4 in Chinese. *Drug Metab Dispos.* 2001;29:268-273.

18. Lamba JK, Lin YS, Thummel K, et al. Common allelic variants of cytochrome P4503A4 and their prevalence in different populations. *Pharmacogenetics.* 2002;12:121-132.

19. Tanabe M, Ieiri I, Nagata N, et al. Expression of P-glycoprotein in human placenta: relation to genetic polymorphism of the multidrug resistance (MDR)-1 gene. *J Pharmacol Exp Ther.* 2001;297:1137-1143.

20. Cascorbi I, Gerloff T, Johne A, et al. Frequency of single nucleotide polymorphisms in the P-glycoprotein drug transporter *MDR1* gene in white subjects. *Clin Pharmacol Ther.* 2001;69:169-174.

21. Kim RB, Leake BF, Choo EF, et al. Identification of functionally variant MDR1 alleles among European Americans and African Americans. *Clin Pharmacol Ther.* 2001;70:189-199.

22. Dai D, Zeldin DC, Blaisdell JA, et al. Polymorphisms in human CYP2C8 decrease metabolism of the anticancer drug paclitaxel and arachidonic acid. *Pharmacogenetics.* 2001;11:597-607.

23. Bahadur N, Leathart JBS, Mutch E, et al. CYP2C8 polymorphisms in Caucasian and their relationship with paclitaxel 6α-hydroxylase

activity in human liver microsomes. *Biochem Pharmacol.* 2002;64:1579-1589.

24. Soyama A, Saito Y, Hanioka N, et al. Non-synonymous single nucleotide alterations found in the CYP2C8 gene result in reduced in vitro paclitaxel metabolism. *Biol Pharm Bull.* 2001;24:1427-1430.

25. Soyama A, Saito Y, Komamura K, et al. Five novel single nucleotide polymorphisms in the *CYP2C8* gene, one of which induces a frame-shift. *Drug Metab Pharmacokinet.* 2002;17:374-377.

26. Dai D, Yang J, Rose R, et al. Identification of variants of CYP3A4 and characterization of their abilities to metabolize testosterone and chlorpyrifos. *J Pharmacol Exp Ther.* 2001;299:825-831.

27. Murayama N, Nakamura T, Saeki M, et al. *CYP3A4* gene polymorphisms influence testosterone 6β-hydroxylation. *Drug Metab Pharmacokinet.* 2002;17:150-156.

28. Belani CP, Kearns CM, Zuhowski EG, et al. Phase I trial, including pharmacokinetic and pharmacodynamic correlations, of combination paclitaxel and carboplatin in patients with metastatic non-small-cell lung cancer. *J Clin Oncol.* 1999;17:676-684.

29. Huizing MT, Giaccone G, van Warmerdam LJ, et al. Pharmacokinetics of paclitaxel and carboplatin in a dose-escalating and dose-sequencing study in patients with non-small-cell lung cancer. The European Cancer Centre. *J Clin Oncol.* 1997;15:317-329.

30. Obasaju CK, Johnson SW, Rogatko A, et al. Evaluation of carboplatin pharmacokinetics in the absence and presence of paclitaxel. *Clin Cancer Res.* 1996;2:549-552.

31. Walle T, Walle UK, Kumar GN, Bhalla KN. Taxol metabolism and disposition in cancer patients. *Drug Metab Dispos.* 1995;23:506-512.

32. Gianni L, Kearns CM, Giani A, et al. Nonlinear pharmacokinetics and metabolism of paclitaxel and its pharmacokinetic/pharmacodynamic relationship in humans. *J Clin Oncol.* 1995; 13:180-190.

33. Ito S, Ieiri I, Tanabe M, Suzuki A, Higuchi S, Otsubo K. Polymorphism of the ABC transporter genes, MDR1, MRP1, MRP2/cMOAT, in healthy Japanese subjects. *Pharmacogenetics.* 2001;11:175-184.

34. Hoffmeyer S, Burk O, von Richter O, et al. Functional polymorphisms of the human multidrug-resistance gene: multiple sequence variations and correlation of one allele with P-glycoprotein expression and activity in vivo. *Proc Natl Acad Sci U S A.* 2000; 97:3473-3478.

Available online at www.sciencedirect.com
SCIENCE DIRECT
Toxicology 216 (2005) 15–23
TOXICOLOGY
www.elsevier.com/locate/toxicol

Detection of autoantibody to aldolase B in sera from patients with troglitazone-induced liver dysfunction

Rawiwan Maniratanachote [a], Ayaka Shibata [a], Shuichi Kaneko [b], Ikuo Yamamori [c], Takanobu Wakasugi [d], Takeshi Sawazaki [e], Kanefusa Katoh [f], Shogo Tokudome [g], Miki Nakajima [a], Tsuyoshi Yokoi [a,*]

[a] *Division of Drug Metabolism, Faculty of Pharmaceutical Sciences, Kanazawa University, Kanazawa 920-1192, Japan*
[b] *Graduate School of Medicine, Kanazawa University, Kanazawa 920-0934, Japan*
[c] *Nagoya First Red-Cross Hospital, Nagoya 453-0046, Japan*
[d] *Fukui Prefectural Hospital, Fukui 910-8526, Japan*
[e] *Hitachi Chemical Co. Ltd., Hitachi 317-8555, Japan*
[f] *Institute for Developmental Research, Aichi Human Service Center, Kasugai, Aichi 480-0392, Japan*
[g] *Dokkyo University School of Medicine, Tochigi 321-0293, Japan*

Received 31 May 2005; received in revised form 13 July 2005; accepted 13 July 2005
Available online 22 August 2005

Abstract

Troglitazone is a thiazolidinedione antidiabetic agent with insulin-sensitizing activities that was withdrawn from the market in 2000 due to its association with idiosyncratic hepatotoxicity. To address the suspected autoantibody production associated with troglitazone, we investigated autoantibodies in sera from patients with type II diabetes mellitus with troglitazone-induced liver dysfunction. Two female patients (47- and 70-year-old) ceased taking troglitazone (400 mg/day) after 23.5 and 16 weeks, respectively, due to increased serum ALT. Using two-dimensional electrophoresis and amino acid sequence analyses, aldolase B was identified as an autoantigen that reacted with antibodies in sera from both patients. The titer of anti-aldolase B remained high for several weeks after stopping troglitazone administration. The mean reactivity of autoantibodies to aldolase B determined by ELISA with sera of patients with chronic hepatitis ($n=40$) and liver cirrhosis ($n=40$) was significantly higher ($p<0.05$ and $p<0.001$, respectively) than with sera of healthy subjects ($n=80$). These findings suggest that liver injury may cause the appearance of autoantibodies to aldolase B which may then aggravate the hepatitis. In addition, the anti-aldolase B titer might indicate the severity of liver dysfunction.

Keywords: Autoantibody; Aldolase B; Troglitazone; Thiazolidinediones; Liver dysfunction

1. Introduction

Adverse drug reactions can be classified into two basic types, reactions that occur directly and can be predicted from the pharmacology of the drug and, in contrast, idiosyncratic reactions which are induced dose-independently and are infrequent and unpredictable. Many idiosyncratic drug reactions have an immunological (hypersensitivity) basis, whereas some are due to a metabolic abnormality of the host (Ju and Uetrecht, 2002; Pirmohamed et al., 1998; Pohl et al., 1988). The liver is an important target for the toxic effects of drugs

* Corresponding author. Tel.: +81 76 234 4407; fax: +81 76 234 4407.
E-mail address: TYOKOI@kenroku.kanazawa-u.ac.jp (T. Yokoi).

0300-483X/$ – see front matter © 2005 Elsevier Ireland Ltd. All rights reserved.
doi:10.1016/j.tox.2005.07.012

because of its essential role in the metabolism of xenobiotic substances. Idiosyncratic drug-induced hepatitis has been assumed to be mediated by immunogens formed by covalent interaction of a reactive drug metabolite with cellular macromolecules (Ju and Uetrecht, 2002; Park et al., 1998). The bioactivated immunogens may not only lead to an immune response directed against the haptenic epitope and the neoantigen, but also against autoantigenic determinants, which is characterized by the formation of autoantibodies (Pohl et al., 1988). A number of hepatotoxic drugs have been reported to produce autoantibodies. For instance, anti-protein disulfide isomerase, anti-microsomal carboxyesterase, anti-calreticulin, anti-ERp72, anti-GRP78, anti-GRP94 and anti-CYP2E1 in halothane hepatitis (Bourdi et al., 1996; Gut et al., 1993; Kenna et al., 1993; Pumford et al., 1993), anti-CYP2C9 in tienilic acid-induced hepatitis (Homberg et al., 1984; Robin et al., 1996), anti-CYP1A2 in dihydralazine-induced hepatitis (Bourdi et al., 1990), and anti-CYPs in aromatic anticonvulsant-induced hypersensitivities (Leeder et al., 1992). However, it is not known whether the autoantibodies are the cause or consequence of the progression of hepatotoxicity. Studies to clarify the possible involvement of autoantibodies in drug-induced hepatitis have been limited, since the appearance of autoantibodies can be seen usually only in human (Descotes, 2000).

Troglitazone (Noscal®, Sankyo, Tokyo, Japan or Rezulin®, Parke-Davis, Morris Plains, NJ) was an early member of the thiazolidinedione chemicals developed for type II diabetes. It has a novel mechanism of action on lowering the blood glucose level by increasing glucose uptake by skeletal muscles, decreasing hepatic glucose production, and sensitizing target tissues to insulin (Fujiwara et al., 1995, 1988; Ciaraldi et al., 1990). However, a rare type of hepatic injury has been reported to be associated with troglitazone therapy. During clinical trials, 1.9% of patients experienced increases in ALT levels greater than three times the upper normal limit (Watkins and Whitcomb, 1998). Fulminant hepatic failure in some patients was reported to occur after long-term troglitazone treatment (more than 4 weeks) (Gitlin et al., 1998; Kuramoto et al., 1998; Neuschwander-Tetri et al., 1998; Shibuya et al., 1998). The hepatic toxicity of troglitazone was not observed in any experimental animals tested including monkey, which has a similar metabolic profile to human (Rothwell et al., 2002; Watanabe et al., 1999). Although the mechanism by which troglitazone causes liver dysfunction in certain individuals is not yet clear, it is thought to be idiosyncratic. There is no report so far of whether a metabolic idiosyncrasy or immunological idiosyncrasy causes this hepatotoxicity.

In the present study, we identified aldolase B as an autoimmune antigen which reacted against antibodies in sera of patients with troglitazone-induced liver dysfunction. The titer of the aldolase B autoantibody remained high for several weeks after stopping troglitazone administration. In addition, we also investigated the formation of the aldolase B autoantibodies in patients with chronic hepatitis and liver cirrhosis as compared with healthy subjects.

2. Materials and methods

2.1. Materials

Biotinylated anti-human IgG, biotinylated anti-rabbit IgG, and a VECTASTAIN ABC kit were purchased from Vector Labolatories Inc. (Burlingame, CA). Prestained SDS–polyacrylamide gel electrophoresis (PAGE) standard of low molecular weight range and prestained isoelectric point (p*I*) marker for two-dimensional PAGE were from Bio-Rad (Hercules, CA). 3,3′-Diaminobenzidine tetrahydrochloride (DAB) and 3,3′,5,5′-tretramethylbenzidine (TMB) liquid substrate system were from Sigma (St. Louis, MO). HRP conjugated anti-human IgA, IgG, IgM, kappa, lambda was from DakoCytomation (Glostrup, Denmark). Immobilon-P membrane was from Millipore (Bedford, UK). Ampholine was from Amersham Biosciences (Buckinghamshire, UK). Purified human aldolase B protein was previously prepared by Haimoto et al. (1989). Recombinant human aldolase B was a generous gift from Prof. Dean R. Tolan (Boston University, Boston, MA). Other chemicals were of the highest grade commercially available.

2.2. Patients

This study was approved by the Ethics Committee of Kanazawa University, Nagoya First Red-Cross Hospital, and Fukui Prefectural Hospital, Japan. The two patients (A and B) gave written informed consent. Serum ALT was periodically measured throughout the time of monitoring. Patient A was a 47-year-old Japanese female with diabetes mellitus. She had been prescribed insulin (36 U/day) for 3 years. Because of inadequate control of the blood sugar level, administration of insulin was stopped and troglitazone therapy (400 mg/day) was started in 1998. Sixteen weeks after the start of troglitazone therapy, the serum ALT level started to increase (32 IU/L). Since the serum ALT level had prominently increased to 229 IU/L at 23.5 weeks, troglitazone therapy was stopped (Fig. 1A). The serum ALT levels gradually decreased (183 IU/L, week 24; 113 IU/L, week 26; 24 IU/L, week 30; 12 IU/L, week 75). Patient B was a 70-year-old Japanese female with diabetes mellitus, hyperlipidemia, and essential hypertension. The patient had been prescribed glibenclamide (10 mg/day), pravastatin (10 mg/day), and celiprolol (100 mg/day). In 1998, because of inadequate control of the blood sugar level, troglitazone therapy was started at

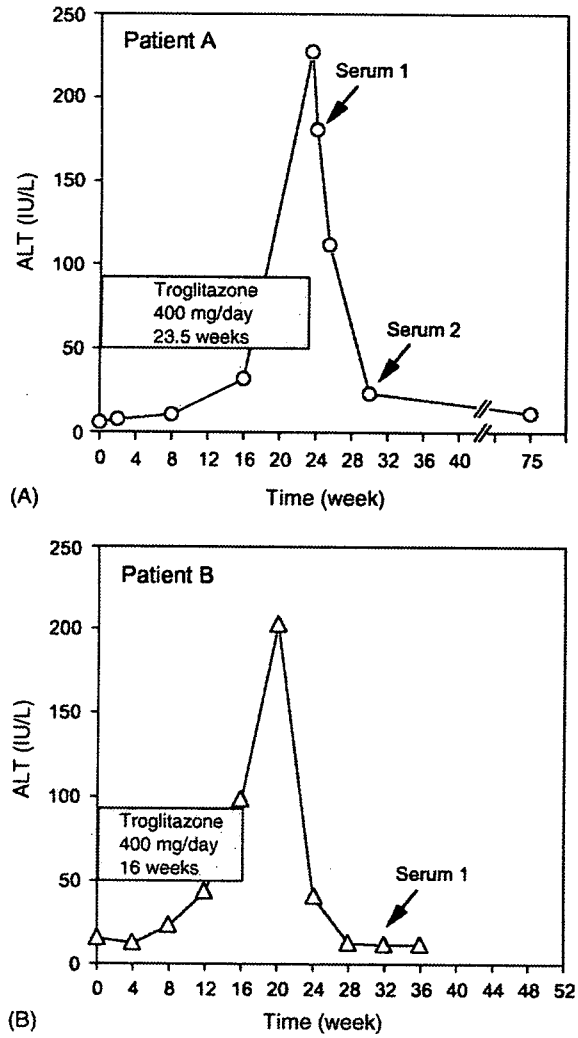

Fig. 1. Changes of serum ALT in patients with troglitazone-induced liver dysfunction. (A) Patient A (female, 47-year-old) and (B) patient B (female, 70-year-old) were administered troglitazone (400 mg/day) for 23.5 and 16 weeks, respectively. During the time of monitoring, the serum ALT of these patients was periodically measured at Fukui Prefectural Hospital and Nagoya First Red-Cross Hospital, Japan. Serum 1 and 2 of patient A and serum 1 of patient B were used in the further study.

400 mg/day. Eight weeks after the start of troglitazone therapy, the serum ALT level started to increase (24 IU/L). Since the serum ALT level continued to increase (44 IU/L, week 12; 99 IU/L, week 16), the troglitazone therapy was stopped (Fig. 1B). Although the serum ALT level had reached 205 IU/L at 20 weeks, the level subsequently decreased to normal (13 IU/L) at week 28.

Serum samples of 80 in-patients with liver dysfunction, 22 males and 18 females with chronic hepatitis, and 18 males and 22 females with liver cirrhosis, were obtained from Kanazawa University Hospital, Kanazawa, Japan. Serum samples of 80 healthy subjects, 45 males and 35 females, were obtained from the Red Cross Blood Supply Center, Kanazawa, Japan. The sera from healthy subjects were negative for serological tests of recent infection with hepatitis A and B viruses, cytomegalovirus and Epstein-Bar virus. All samples were stored at −20 °C until analysis.

2.3. Preparation of liver subcellular fractions

For immunoblot analysis, human liver samples were obtained from autopsy. The use of the human liver for the study was approved by the Ethics Committee of Dokkyo University School of Medicine (Tochigi, Japan). Liver tissues were rapidly frozen in liquid nitrogen immediately after excision and were stored at −80 °C. Human liver samples from two individuals (54-year-old male and 60-year-old female, ischemia cardionecrosis) were homogenized with 3 volumes of 0.1 M Tris–HCl (pH 7.4), 0.1 M KCl and 1 mM EDTA. Nuclei fractions were isolated by centrifugation at 600 × *g* for 10 min. The supernatant was centrifuged at 9000 × *g* for 20 min to isolate the mitochondria fraction. The supernatant was centrifuged at 105,000 × *g* for 60 min to prepare the microsome and cytosol fractions. The prepared fractions of nuclei, mitochondria, and microsomes were washed two times using the same experimental procedures. The protein concentration was measured according to the method of Lowry et al. (1951) with bovine serum albumin as a standard. The prepared subcellular fractions were stored at −80 °C until use.

2.4. Sodium dodecyl sulphate–polyacrylamide gel electrophoresis (SDS–PAGE) and immunoblot analysis

SDS–PAGE and immunoblot analysis were carried out. In brief, human liver homogenates (20 μg), nuclei (10 μg), mitochondria (10 μg), microsomes (10 μg), and cytosol (10 μg) were applied to 7.5% polyacrylamide gel. Proteins were transferred to an Immobilon-P membrane. The membrane was incubated with serum from healthy subjects, patient A or B (diluted 1:100) as the first antibody at 37 °C for 60 min. Subsequently, the membrane was incubated with biotinylated anti-human immunoglobulin (diluted 1:2000) at 37 °C for 30 min and incubated with avidin–biotin complex (VECTASTAIN ABC kits) at 37 °C for 30 min. Anti-sera to the human aldolase B raised in rabbit as described previously (Haimoto et al., 1989) was used (final concentration: 0.1 μg/ml) at 37 °C for 30 min. The membrane was incubated with biotinylated anti-rabbit IgG (diluted 1:2000) at 37 °C for 20 min and then with avidin–biotin complex (VECTASTAIN ABC kit) at 37 °C for 20 min. 3,3′-Diaminobenzidinetetrahydrochloride (DAB) was used as a substrate for peroxidase.

2.5. Two-dimensional electrophoresis

Two-dimensional electrophoresis was carried out according to the method described by O'Farrell (1975) with slight modifications. Isoelectric focusing (IEF) gel was prepared from a mixture containing 8 M urea, 2% Nonidet P-40, 2% Ampholines carrier ampholites (0.5% pH 6.0–8.0 range, 1.5% pH

7.0–9.0 range), and 4% acrylamide. Prefocusing was carried out at 200 V for 15 min, 300 V for 20 min, and then 400 V for 20 min. Samples up to 50 μl in volume were subjected to electrophoresis at 400 V for 12–16 h and at 800 V for 1 h using 0.02 M NaOH at the anode and 0.01 M H_3PO_4 at the cathode. The second dimensional separation was carried out using the 7.5% SDS–PAGE as described above.

2.6. Amino acid sequence analysis

After the two-dimensional electrophoresis, the separated proteins were visualized by staining with Coomassie Brilliant Blue G-250 (CBB). The corresponding spots of interest were compared with the profile from the immunoblotting with the patient A serum sample. The stained 40 kDa spots with *pI*s of 7.4 and 7.6 were excised and subjected to trypsin digestion. The analysis of peptides was carried out at APRO Science Inc. (Tokushima, Japan) by nanoflow ESI on a Q-TOF mass spectrometer.

2.7. Enzyme-linked immunosorbent assay (ELISA)

The sera of patient A (serum 2), the healthy subjects ($n = 80$), and those with chronic hepatitis ($n = 40$) and liver cirrhosis ($n = 40$) were subjected to ELISA. Recombinant human aldolase B purified from *E. coli* DH5α expressing cells was used as an antigen. To avoid non-specific reactions with the bacterial antigens, all human sera were pre-absorbed with *E. coli* DH5α lysate 1:2 (v/v) for 4 h at room temperature with agitation and were centrifuged at 10,000 rpm for 15 min at 4 °C.

Hundred microlitres of human recombinant aldolase B (10 μg/ml) in carbonate/bicarbonate buffer, pH 9.6 were coated onto each well of flat-bottomed microtiter plates (Corning, NY) and incubated overnight at 4 °C. The wells were washed three times with wash solution (50 mM Tris, 0.14 M NaCl, 0.05% Tween 20, pH 8.0) and blocked with 150 μl of solution containing 50 mM Tris–HCl, 0.14 M NaCl and 1% BSA, pH 8.0, at 37 °C for 2 h. After washing three times, 100 μl of sera (1:100) in the solution containing 50 mM Tris–HCl, 0.14 M NaCl, 0.1% BSA and 0.05% Tween 20, pH 8.0, were applied to each well and incubated at 37 °C for 1 h. Each plate included serum from patient A as a positive control. The wells were washed three times before adding HRP conjugated anti-human IgA, IgG, IgM, kappa, lambda (1:8000) in the same solution as for the serum dilution. The wells were incubated at 37 °C for 1 h, washed five times and 100 μl of tetramethyl benzidine (TMB) substrate solution were added to each well. After 30 min of incubation, the TMB reaction was stopped by adding 100 μl of 2 M H_2SO_4. The optical density was read at 450 nm by using a microtiter plate reader (Biotrak II, Amersham Biosciences). Controlled wells that were coated without aldolase B were also used for each serum sample. All assays were performed in triplicate and the specific binding of antibody to aldolase B in sera was calculated by subtracting the average absorbance of the control wells from the average absorbance of the aldolase B coated wells.

2.8. Statistical analysis

Data from ELISA were analyzed by Kruskal–Wallis nonparametric analysis of variance (ANOVA) followed by Dunn's multiple comparison test. $p < 0.05$ was considered significant.

3. Results

Immunoblot analyses were performed with human liver subcellular fractions using sera from healthy subjects and patients A and B. In order to investigate the existance of troglitazone-induced autoantibodies and to elucidate the subcellular localization of antigen proteins, human liver subcellular fractions from two different individuals were subjected to SDS–PAGE. Immunoblot analysis was performed using sera 1 of patients A and B (Fig. 1) as the first antibody. Immunostained bands of 55 kDa and 49 kDa molecular weight were observed in the serum of a healthy subject. The 55 kDa band was more intense than the 49 kDa band (Fig. 2). These bands could be detected in the sera of all healthy subjects examined ($n = 8$, data not shown). The serum of patient A recognized an intense band of 40 kDa and a faint band of 45 kDa in the cytosolic fraction, whereas a faint band of 40 kDa was detected with the serum of patient B (Fig. 2). The serum of a healthy control could not detect these 40 kDa and 45 kDa bands. Other minor bands in patients A and B sera showed low reproducibility. Thus,

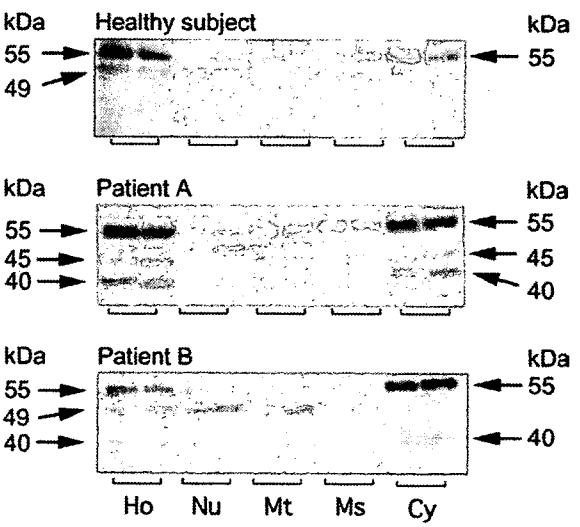

Fig. 2. Immunoblot analyses for human liver subcellular fractions using sera from healthy controls and patients A and B. Human liver homogenates (Ho), nuclei (Nu), mitochondria (Mt), microsomes (Ms), and cytosol (Cy) from two different individuals were subjected to SDS–PAGE. Immunoblot analyses were performed using sera from a healthy subject (1:100), patients A (serum 1, 1:100) and B (serum 1, 1:100) as the first antibody as described in Section 2.

we focused on the identification of the 40 kDa antigenic protein in further experiments.

In the serum of patient A, the immunoglobulin subtypes of antibody detecting the 55 kDa, 49 kDa, 45 kDa and 40 kDa proteins were IgG, IgM, IgG and IgG, respectively (data not shown). In the serum of patient B, the 55 kDa, 49 kDa and 40 kDa proteins were IgG, IgM and IgM, respectively (data not shown).

3.1. Two-dimensional electrophoresis of human liver cytosol and immunoblot analysis with the serum of patient A as the first antibody

To identify the 40 kDa antigenic protein, two-dimensional electrophoresis was carried out to analyze the liver cytosolic proteins. The separated proteins were stained with CBB (Fig. 3A). A relatively small number of protein spots were detectable due to the narrow pH range (pH 6–9) employed for the IEF. Immunoblot analysis using serum 1 of patient A as the first antibody indicated the presence of three 40 kDa antigenic proteins, whose estimated p*I*s were 7.6, 7.4 and 7.2 (Fig. 3B). The other immunostained spots seen on the membrane were assumed to be due to non-specific or non-immunological reactions with the serum. Spots of 55 kDa and 49 kDa were also observed on the immunostained membrane with the sera from the healthy subjects (data not shown).

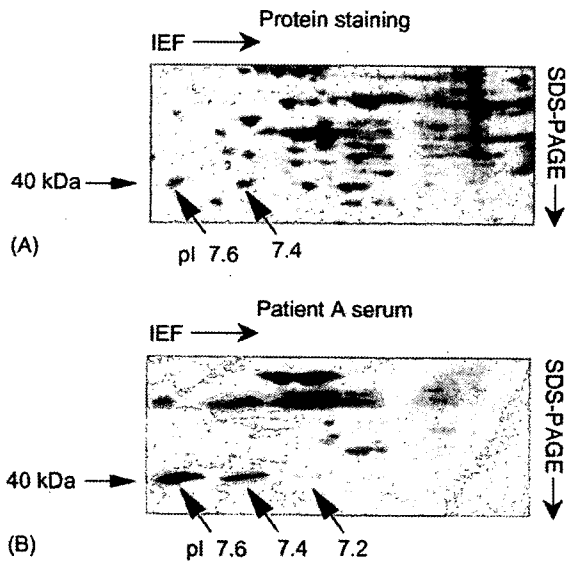

Fig. 3. Two-dimensional electrophoresis and immunoblot analyses using serum from patient A. Human liver cytosol (230 μg) was separated by two-dimensional electrophoresis. (A) The gel was stained with CBB. (B) Immunoblot analyses were performed using the serum 1 from patient A (1:100) as the first antibody as described in Section 2. The approximate p*I*s on the two-dimensional PAGE gel are indicated.

3.2. Identification of the 40 kDa antigenic protein

Two of the three immunoreactive spots with p*I*s of 7.6 and 7.4 in Fig. 3 were excised from the protein-stained two-dimensional PAGE gel and subjected to trypsin digestion. Amino acid sequencing was carried out with nanoflow ESI on a Q-TOF mass spectrometer. A 15-amino acid sequence (GGKAANKEATQEAFM) was identified from the trypsin-treated fragment of both spots. This sequence was perfectly matched with the amino acid sequence from 315 to 329 (GGKAANKEATQEAFM) of human aldolase B.

3.3. Confirmation of aldolase B by immunoblot analyses

To confirm that the 40 kDa protein was aldolase B, the following experiments were performed. To examine the possibility that the serum of patient A contained an antibody to aldolase B, purified human aldolase B protein (40 kDa) of 3 μg, 1 μg, and 0.25 μg were applied to SDS–PAGE and subsequently transferred to Immobilon-P membrane and immunostained with the serum of patient A as the first antibody. The serum 1 of patient A recognized the aldolase B in a concentration-dependent manner (Fig. 4A). The other serum of patient A (serum 2) and that of patient B (serum 1) showed the same immunological recognition of the purified aldolase B protein as that of serum 1 from patient A (data not shown).

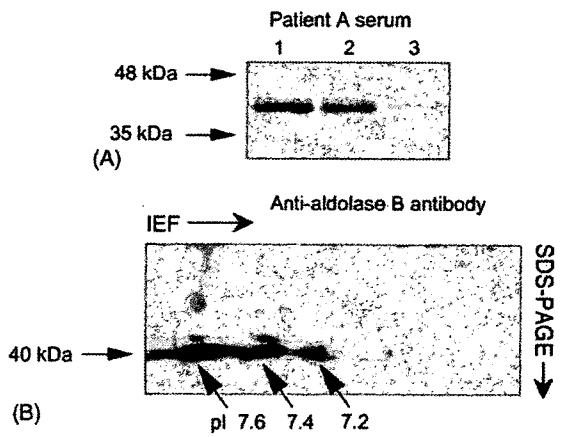

Fig. 4. Immunoblot analyses to confirm the occurrence of anti-aldolase B antibody. (A) Purified aldolase B protein at 3 μg (lane 1), 1 μg (lane 2), and 0.25 μg (lane 3) was subjected to SDS–PAGE. Immunoblot analysis was performed using serum 1 of patient A (1:100) as the first antibody. (B) Human liver cytosol (230 μg) was separated by two-dimensional electrophoresis. Immunoblot analysis was performed using anti-human aldolase B antibody as the first antibody as described in Section 2.

To examine the possibility that the spots recognized by immunostaining with the serum of patient A were derived from aldolase B, anti-human aldolase B antibody was applied instead of the serum of patient A to the liver cytosol prepared by two-dimensional PAGE. Three distinct spots with approximate p*I*s of 7.6 and 7.4, and 7.2, appeared (Fig. 4B). No other major spot was recognized by the anti-human aldolase B antibody. These spots showed the same p*I*s and molecular weights as the spots demonstrated by the serum of patient A.

To evaluate the titer of anti-aldolase B autoantibody in the sera of patients A and B the Immobilon-P membrane was employed to transfer the purified human aldolase B protein (1 μg). Immuoblot experiments were performed with the diluted sera from the patients. The sera 1 and 2 (23.5-week after stopping troglitazone therapy) of patient A showed titers of 1:3200 and 1:6400, respectively (data not shown). The titer of serum 1 (16-week after stopping troglitazone therapy) of patient B was 1:1600 (data not shown).

3.4. Determination of anti-aldolase B autoantibodies in sera of patients with liver diseases

The sera of the patients with liver diseases were examined by ELISA to determine whether the anti-aldolase B antibody appeared in association with the liver diseases. Fig. 5A shows the individual anti-aldolase B antibody in sera from the healthy subjects ($n=80$) and chronic hepatitis ($n=40$) and liver cirrhosis ($n=40$) patients. Anti-aldolase B autoantibodies in the chronic hepatitis and liver cirrhosis patients were significantly higher

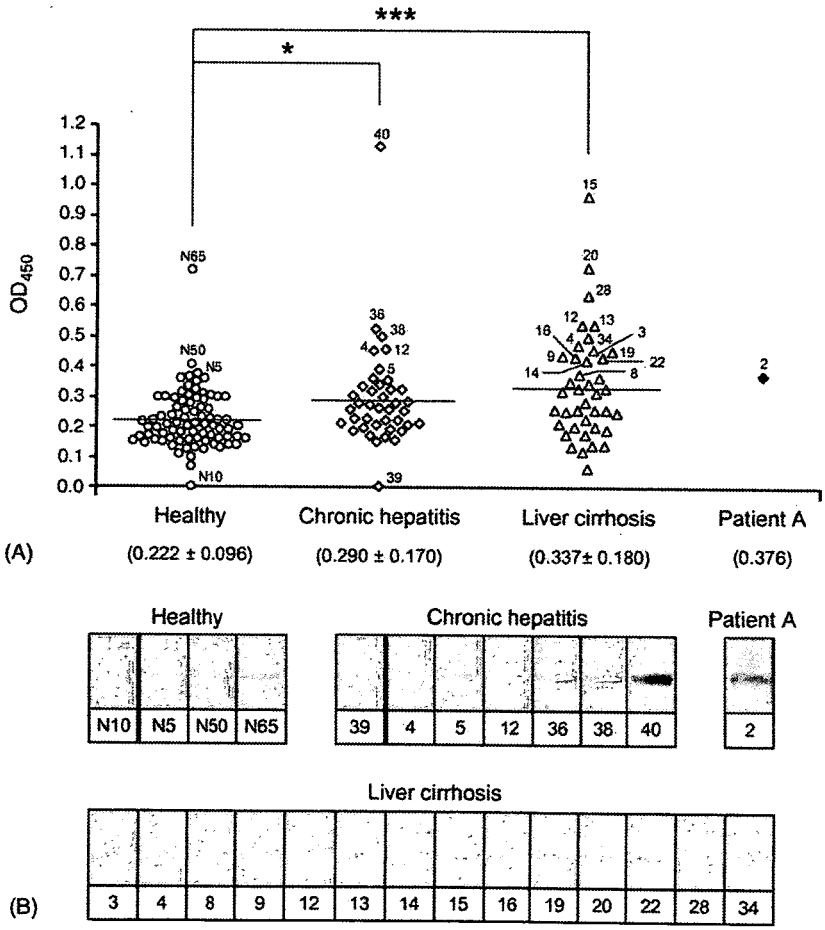

Fig. 5. Identification of autoantibodies reacting with aldolase B in sera from patients with liver diseases. (A) Sera of healthy subjects ($n=80$), chronic hepatitis ($n=40$) and liver cirrhosis ($n=40$) as well as patient A (positive control) were investigated for anti-aldolase B autoantibodies by ELISA as described in Section 2. The horizontal bar represents the average value of each group. The means ± S.D. are indicated in parentheses. $^{*}p<0.05$, $^{***}p<0.001$ compared with the control. (B) Immunoblot analyses of anti-aldolase B autoantibody positive sera. The sera which showed an OD_{450} higher than that of patient A, as well as negative sera from a healthy subject and chronic hepatitis, N10 and N39, respectively, were subjected to immunoblot analyses. The numbers correspond to the subjects indicated in (A).

than those in the healthy subjects ($p < 0.05$ and $p < 0.001$, respectively). Using serum 2 of patient A as a reference, all sera having an OD_{450} higher than that of patient A as well as negative sera from healthy subjects and those with chronic hepatitis, N10 and 39, respectively, were subjected to immunoblot analysis. Except the negative sera, all sera which showed positive reactivity by ELISA also showed a single positive band of aldolase B by immunoblotting (Fig. 5B).

4. Discussion

Idiosyncratic adverse reactions are difficult to study because of their rare occurrence, dose-independence and lack of reproducibility in animal models. There are two classes of reactions, metabolic and immunologic idiosyncrasy. The later class is thought to be responsible for most adverse drug reactions (Ju and Uetrecht, 2002; Pirmohamed et al., 1998; Pohl et al., 1988). In the present study, troglitazone-induced liver dysfunction was investigated in terms of the autoantibody formation. Two patients (A and B) who received troglitazone 400 mg/day showed increases of serum ALT (Fig. 1A and B), which indicated an abnormality of liver function. The sera of both patients reacted prominently against troglitazone-induced neoantigens in the cytosol subfraction (Fig. 2) which were identified as aldolase B (EC 4.1.2.13). Schapira et al. (1977) reported the microheterogeneity of human liver aldolase B, which shows 5 bands by IEF according to tetramers formed by two types of aldolase B chains, β and β′. The β′ chain is the result of a post-transcriptional modification by the deamidation of β chain. In our study, the spots of the two-dimensional PAGE at p*I* 7.6, 7.4, and 7.2 might be consistent with the β^4, $\beta^3\,\beta'$ and $\beta^2\,\beta'^2$ chains, respectively (Fig. 3). In mammal, three isoenzymes of aldolase (A–C) have been classified (Penhoet et al., 1966; Rutter, 1964). They are distinguished by their different activity towards the two substrates of fructose 1,6-diphospate and fructose 1-phosphate (Rutter et al., 1961). Aldolase B is predominantly localized in liver and kidney, while aldolase A and C are mainly localized in muscle and in brain, respectively (Penhoet et al., 1966; Rutter, 1964).

The mechanism by which autoantibodies are formed is still incompletely understood. Hepatic microsomal cytochrome P450 (CYP) isoforms such as CYP1A2, CYP2A6, CYP2B6, and CYP2E1 have been extensively studied as autoantigens in many liver diseases including viral, autoimmune and drug-induced hepatitis (Park et al., 1998; Manns and Obermayer-Straub, 1997). Although how these CYPs become autoimmune targets is still unknown, the findings of these studies reflected the major metabolic role of CYPs in the liver. However, in our findings no prominent band of CYPs could be detected in the microsomal subfraction of troglitazone-treated patient sera that was distinct from those in the sera of healthy subjects.

There is evidence that the metabolic activation of some drugs can result in the formation of chemically reactive metabolites that bind to macromolecules in the cell, unless adequately detoxified, leading to several pathological effects including hypersensitivities (Park et al., 1998). Thus, an imbalance between metabolic activation and detoxification in some individuals may lead to idiosyncratic adverse drug reactions. Troglitazone is metabolized by many enzymes in the liver including CYP3A4 and CYP2C8 which generated a quinone-type metabolite, troglitazone quinone (Tettey et al., 2001; Yamazaki et al., 1999). Based on the general involvement of quinones in cytotoxicity, troglitazone quinone has been proposed to have an association with troglitazone-induced hepatotoxicity (Neuschwander-Tetri et al., 1998). Aldolase B, which is an enzyme predominantly localized in the liver (Penhoet et al., 1966), may be one of the target proteins that interact with reactive species generated by troglitazone and trigger the immune response. Based on the detoxification enzyme in phase II, which is responsible for eliminating toxic metabolites before the generation of neoantigens, a recent report has shown that the double null genotype of *GSTM*1 and *GSTT*1 is associated with an abnormal elevation of liver enzymes caused by troglitazone treatment (Watanabe et al., 2003). This may suggest that idiosyncratic drug reactions might be the consequence of a complex genetic basis involving numerous processes.

In order to investigate whether the formation of anti-aldolase B was specific for troglitazone-induced hepatotoxicity, the sera of patients with liver diseases, chronic hepatitis and liver cirrhosis, were also examined. According to the etiology, chronic hepatitis results from several causes such as autoimmune reactions, viral hepatitis B–D, drugs, Wilson's disease, α-1-antitrypsin disease as well as unknown causes, whereas cirrhosis is considered to be the advanced stage of hepatitis (Batts and Ludwig, 1995; Jevon, 2001). As shown in Fig. 5, the mean reactivity of autoantibodies to aldolase B in the patient sera with liver diseases was also significantly higher than that in the healthy subjects. The average ALT level in chronic hepatitis and cirrhosis was 39.50 ± 15.7 IU/L ($n = 40$) and 52.35 ± 28.70 IU/L ($n = 40$), respectively (data not shown) which correlated with the titer of autoantibodies to aldolase B. Brown et al. (1987) reported that the presence of autoantibodies to aldolase in patients with hepatitis A, B, non-A/non-B,

and those who were hepatitis B surface antigen positive or had autoimmune hepatitis was higher than in healthy subjects. In that study, rabbit muscle aldolase, which is referred to as aldolase A (Penhoet et al., 1966), was used. According to the high homology between aldolase A and B, only the amino acid sequence 357–362 is recognized as a non-conserved residue that enables the classification of the mammalian aldolase (Rutter, 1964). The amino acid sequence 315–329 of aldolase B was identified in our study. Therefore, our findings were remarkably consistent with those of a previous report (Brown et al., 1987). In addition, we included the data of autoantibodies to aldolase B detected in troglitazone-induced hepatitis as well as those in liver cirrhosis.

At present, the exact mechanism involved in the formation of autoantibodies is unknown. There is a possibility that, after cellular injury, intracellular antigens might be seen as non-self by the immune system and result in the stimulation of an immune response toward cryptic epitopes on the antigens (Lanzavecchia, 1995). Accumulating evidence suggests that liver damage may cause the production of autoantibodies to aldolase B and that the severity of hepatitis may be estimated by the antibody titer.

In conclusion, aldolase B was identified as an autoimmune antigen in patients with troglitazone-induced liver dysfunction. This finding is the first evidence that troglitazone-induced hepatitis may have an immunological basis. In addition, the elevation of anti-aldolase B autoantibody in sera is likely a common phenomenon associated with hepatitis. This autoantibody may play an essential role in aggravating the liver dysfunction. Further studies will be needed to clarify the mechanisms of idiosyncratic adverse drug reactions.

Acknowledgements

We thank Prof. Dean R. Tolan, Boston University, Boston, MA, for providing recombinant human aldolase B. We also thank Mr. Brent Bell for reviewing the manuscript. This work was supported in part by a grant from the Ministry of Education, Science, Sports and Culture of Japan, and by Research on Advanced Medical Technology, Health and Labor Science Research Grants from the Ministry of Health, Labor and Welfare of Japan.

References

Batts, K.P., Ludwig, J., 1995. Chronic hepatitis. An update on terminology and reporting. Am. J. Surg. Pathol. 19, 1409–1417.

Bourdi, M., Chen, W., Peter, R.M., Martin, J.L., Buters, J.T., Nelson, S.D., Pohl, L.R., 1996. Human cytochrome P450 2E1 is a major autoantigen associated with halothane hepatitis. Chem. Res. Toxicol. 9, 1159–1166.

Bourdi, M., Larrey, D., Nataf, J., Bernuau, J., Pessayre, D., Iwasaki, M., Guengerich, F.P., Beaune, P.H., 1990. Anti-liver endoplasmic reticulum autoantibodies are directed against human cytochrome P-450IA2. A specific marker of dihydralazine-induced hepatitis. J. Clin. Invest. 85, 1967–1973.

Brown, C., Toh, B.H., Pedersen, J.S., Clarke, F.M., Mackay, I.R., Gust, I., 1987. Autoantibody to aldolase in acute and chronic hepatitis. Pathology 19, 347–350.

Ciaraldi, T.P., Gilmore, A., Olefsky, J.M., Goldberg, M., Heidenreich, K.A., 1990. In vitro studies on the action of CS-045, a new antidiabetic agent. Metabolism 39, 1056–1062.

Descotes, J., 2000. Autoimmunity and toxicity testing. Toxicol. Lett. 112–113, 461–465.

Fujiwara, T., Okuno, A., Yoshioka, T., Horikoshi, H., 1995. Suppression of hepatic gluconeogenesis in long-term troglitazone treated diabetic KK and C57BL/KsJ-db/db mice. Metabolism 44, 486–490.

Fujiwara, T., Yoshioka, S., Yoshioka, T., Ushiyama, I., Horikoshi, H., 1988. Characterization of new oral antidiabetic agent CS-045: Studies in KK and ob/ob mice and Zucker fatty rats. Diabetes 37, 1549–1558.

Gitlin, N., Julie, N.L., Spurr, C.L., Lim, K.N., Juarbe, H.M., 1998. Two cases of severe clinical and histologic hepatotoxicity associated with troglitazone. Ann. Intern. Med. 129, 36–38.

Gut, J., Christen, U., Huwyler, J., 1993. Mechanisms of halothane toxicity: novel insights. Pharmacol. Ther. 58, 133–155.

Haimoto, H., Kurobe, N., Hosoda, S., Kato, K., 1989. Sensitive enzyme immunoassay for human aldolase B. Clin. Chim. Acta 181, 27–36.

Homberg, J.C., Andre, C., Abuaf, N., 1984. A new anti-liver-kidney microsome antibody (andi-LKM2) in tienilic acid-induced hepatitis. Clin. Exp. Immunol. 55, 561–570.

Jevon, G.P., 2001. Grade and stage in chronic hepatitis. Pediatr. Dev. Pathol. 4, 372–380.

Ju, C., Uetrecht, J.P., 2002. Mechanism of idiosyncratic drug reaction: relative metabolites formation, protein binding and the regulation of the immune system. Curr. Drug Metab. 3, 367–377.

Kenna, J.G., Knight, T.L., van Pelt, F.N.A.M., 1993. Immunity to halothane metabolite-modified proteins in halothane hepatitis. Ann. N. Y. Acad. Sci. 685, 646–661.

Kuramoto, K., Shimizu, N., Toda, G., 1998. Liver dysfunction associated with troglitazone (Noscal®). Rinsho-Iyaku 14, 461–466.

Lanzavecchia, A., 1995. How can cryptic epitopes trigger autoimmunity? J. Exp. Med. 181, 1945–1948.

Leeder, J.S., Riley, R.J., Cook, V.A., Spielberg, S.P., 1992. Human anti-cytochrome P450 antibodies in aromatic anticonvulsant-induced hypersensitivity reactions. J. Pharmacol. Exp. Ther. 263, 360–367.

Lowry, O.H., Rosebrough, N.J., Farr, A.L., Randall, R.J., 1951. Protein measurement with the Folin phenol reagent. J. Biol. Chem. 193, 265–275.

Manns, M.P., Obermayer-Straub, P., 1997. Cytochromes P450 and uridinetriphosphate-glucuronosyltransferases: model autoantigens to study drug-induced, virus-induced and autoimmune liver disease. Hepatology 26, 1054–1066.

Neuschwander-Tetri, B.A., Isley, W.L., Oki, J.C., Ramrakhiani, S., Quiason, S.G., Phillips, N.J., Brunt, E.M., 1998. Troglitazone-induced hepatic failure leading to liver transplantation. Ann. Intern. Med. 129, 38–41.

O'Farrell, P.H., 1975. High resolution two-dimensional electrophoresis. J. Biol. Chem. 250, 4007–4021.

Park, B.K., Pirmohamed, M., Kitteringham, N.R., 1998. Role of drug disposition in drug hypersensitivity: a chemical, molecular and clinical perspective. Chem. Res. Toxicol. 11, 969–988.

Penhoet, E., Rajkumar, T., Rutter, W.J., 1966. Multiple forms of fructose diphosphate aldolase in mammalian tissues. Proc. Natl. Acad. Sci. U.S.A. 56, 1275–1282.

Pirmohamed, M., Breckenridge, A.M., Kitteringham, N.R., Park, B.K., 1998. Adverse drug reactions. Br. Med. J. 316, 1295–1298.

Pohl, L.R., Satoh, H., Christ, D.D., Kenna, J.G., 1988. The immunologic and metabolic basis of drug hypersensitivities. Ann. Rev. Pharmacol. 28, 367–387.

Pumford, N.R., Martin, B.M., Thomassen, D., Burris, J.A., Kenna, J.G., Martin, J.L., Pohl, L.R., 1993. Serum antibodies from halothane hepatitis patients react with the rat endoplasmic reticulum protein Erp72. Chem. Res. Toxicol. 6, 609–615.

Robin, M.A., Maratrat, M., Le Roy, M., Le Breton, F.P., Bonierbale, E., Dansette, P., Ballet, F., Mansuy, D., Pessayre, D., 1996. Antigenic targets in tienilic acid hepatitis: Both cytochrome P450 2C11 and 2C11-tienilic acid adducts are transported to the plasma membrane of rat hepatocytes and recognized by human sera. J. Clin. Invest. 98, 1471–1480.

Rothwell, C., McGuire, E.J., Altrogge, D.M., Masuda, H., de la Iglesia, F.A., 2002. Chronic toxicity in monkeys with the thiazolidinedione antidiabetic agent troglitazone. J. Toxicol. Sci. 27, 35–47.

Rutter, W.J., 1964. Evolution of aldolase. Fed. Proc. 23, 1248–1257.

Rutter, W.J., Richards, O.C., Woodfin, B.M., 1961. Comparative studies of liver and muscle aldolase. I. Effect of carboxypeptidase on catalytic activity. J. Biol. Chem. 236, 3193–3197.

Schapira, F., Gregori, C., Hatzfeld, A., 1977. Isoelectrofocusing of aldolase B from normal human livers and from livers with hereditary fructose intolerance. Clin. Chim. Acta 78, 1–8.

Shibuya, A., Watanabe, M., Fujita, Y., Saigenji, K., Kuwao, S., Takahashi, H., Takeuchi, H., 1998. An autopsy case of troglitazone-induced fulminant hepatitis. Diabetes Care 21, 2140–2143.

Tettey, J.N., Maggs, J.L., Rapeport, W.G., Pirmohamed, M., Park, B.K., 2001. Enzyme induction dependent bioactivation of troglitazone and troglitazone quinone in vivo. Chem. Res. Toxicol. 14, 965–974.

Watanabe, I., Tomita, A., Shimizu, M., Sugawara, M., Yasumo, H., Koishi, R., Takahashi, T., Miyoshi, K., Nakamura, K., Izumi, T., Matsushita, Y., Furukawa, H., Haruyama, H., Koga, T., 2003. A study to survey susceptible genetic factors responsible for troglitazone-associated hepatotoxicity in Japanese patients with type 2 diabetes mellitus. Clin. Pharmacol. Ther. 73, 435–455.

Watanabe, T., Ohashi, Y., Yasuda, M., Takaoka, M., Furukawa, T., Yamoto, T., Sanbuissho, A., Manabe, S., 1999. Was it possible to predict liver dysfunction caused by troglitazone during the non-clinical safety studies? Iyakuhin Kenkyu 30, 537–546.

Watkins, P.B., Whitcomb, R.W., 1998. Hepatic dysfunction associated with troglitazone. N. Engl. J. Med. 338, 916–917.

Yamazaki, H., Shibata, A., Suzuki, M., Nakajima, M., Shimada, N., Guengerich, F.P., Yokoi, T., 1999. Oxidation of troglitazone to a quinone-type metabolite catalyzed by cytochrome P-450 2C8 and P-450 3A4 in human liver microsomes. Drug Metab. Dispos. 27, 1260–1266.

Drug Metab. Pharmacokinet. 20 (2): 135-143 (2005).

Regular Article

Urinary Excretion of Phenytoin Metabolites, 5-(4′-hydroxyphenyl)-5-Phenylhydantoin and its O-glucuronide in Humans and Analysis of Genetic Polymorphisms of UDP-glucuronosyltransferases

Hiroyuki YAMANAKA[1], Miki NAKAJIMA[1], Yusuke HARA[2], Miki KATOH[1], Osamu TACHIBANA[3], Junkoh YAMASHITA[3] and Tsuyoshi YOKOI[1]

[1]*Drug Metabolism and Toxicology, Division of Pharmaceutical Sciences, Graduate School of Medical Science, Kanazawa University, Kanazawa, Japan*
[2]*Kanazawa University Hospital, Kanazawa, Japan*
[3]*Department of Neurosurgery, Division of Neuroscience, Graduate School of Medical Science, Kanazawa University, Kanazawa, Japan*

Full text of this paper is available at http://www.jssx.org

Summary: The anticonvulsant agent phenytoin (5,5-diphenylhydantoin) is mainly excreted as 5-(4′-hydroxyphenyl)-5-phenylhydantoin (4′-HPPH) *O*-glucuronide in humans. Previously, we demonstrated that the glucuronidation of 4′-HPPH is catalyzed by multiple UDP-glucuronosyltransferases (UGTs) of UGT1A1, UGT1A4, UGT1A6, and UGT1A9. Since 4′-HPPH may be bioactivated to a reactive metabolite by peroxidase, the glucuronidation in considered to be a detoxification pathway. In the present study, we investigated the relationship between the extent of interindividual variability in the urinary excretion levels of 4′-HPPH and its *O*-glucuronide and genotyping of *CYP2C9*, *CYP2C19*, *UGT1A1*, *UGT1A6*, and *UGT1A9*. 4′-HPPH and its glucuronide in urine samples from 15 patients to whom phenytoin was administered were measured by liquid chromatography-tandem mass spectrometry. When the molar ratio of 4′-HPPH *O*-glucuronide/4′-HPPH was calculated as an index of glucuronidation, a large interindividual variability (11 fold) was observed in the 15 patients. Phenytoin is metabolized to 4′-HPPH by CYP2C9 and CYP2C19 in which there are genetic polymorphisms. Although 5 patients were genotyped as heterozygotes of mutated alleles of *CYP2C9* or *CYP2C19* genes, no relationship with the interindividual difference in the total excretion levels of 4′-HPPH and its *O*-glucuronide was observed. The *UGT1A1*6*, *UGT1A1*28*, *UGT1A1*60* and *UGT1A6*2* alleles were found in 1, 3, 6, and 8 patients, respectively. Although there was no relationship between the genetic polymorphisms of UGT1As and the interindividual difference in the 4′-HPPH glucuronidation, the large interindividual variability of 4′-HPPH glucuronidation may contribute to interindividual differences in toxic reactions to phenytoin.

Key words: Cytochrome P450; UDP-glucuronosyltransferase; genetic polymorphism; interindividual difference

Introduction

Phenytoin (5,5-diphenylhydantoin) is a widely used anticonvulsant drug. Hypersensitivity reactions induced by phenytoin occur in 5 to 10% of patients.[1] The relationship between the phenytoin dose and the resulting concentration in the serum varies markedly between individuals for reasons not fully clarified. Because of its narrow therapeutic range (10–20 μg/mL) and nonlinearity in the blood concentration,[2] therapeutic drug monitoring is usually recommended. This drug undergoes extensive metabolic conversion in the liver, with <5% of an administered dose being excreted in the urine in the unchanged form.[3] Phenytoin is mainly metabolized to 5-(4′-hydroxyphenyl)-5-phenylhydantoin (4′-HPPH) (**Fig. 1**). The formation of 4′-HPPH is catalyzed mainly by cytochrome P450 (CYP) 2C9, and to a minor extent, by CYP2C19 in humans.[4,5] 4′-

Received; December 22, 2004, Accepted; March 4, 2005
To whom correspondence should be addressed: Tsuyoshi YOKOI, Ph.D., *Drug Metabolism and Toxicology, Division of Pharmaceutical Sciences, Graduate School of Medical Science, Kanazawa University, Kanazawa, Japan. Tel. & Fax. +81-76-234-4407, E-mail: TYOKOI@kenroku.kanazawa-u.ac.jp*

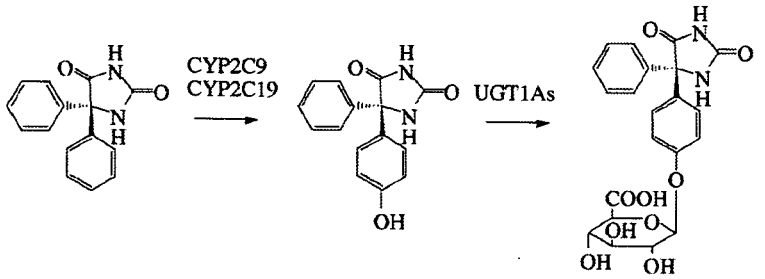

Fig. 1. Major metabolic pathways of phenytoin in humans.

HPPH is present in plasma almost entirely as a glucuronic acid conjugate. Some 75% of administered phenytoin appear in urine as 4′-HPPH *O*-glucuronide.[6] Since 4′-HPPH alternatively may be bioactivated by peroxidase to a reactive intermediate, which can oxidize lipids, proteins, and DNA,[7-9] the glucuronidation may prevent competing bioactivation of 4′-HPPH to a toxic reactive intermediate.

The glucuronidation of endogenous compounds and xenobiotics is catalyzed by UDP-glucuronosyltransferases (UGTs) which compose a superfamily. UGTs exist as two families, UGT1 and UGT2. UGT1 isoforms are produced by alternative splicing of the *UGT1* gene complex. Recently, we reported that multiple UGT1A isoforms (UGT1A1, UGT1A4, UGT1A6, and UGT1A9) are involved in the glucuronosyltransferase activity of 4′-HPPH in humans.[10] Furthermore, a large interindividual difference in the glucuronosyltransferase activity of 4′-HPPH was shown in liver microsomes from 14 humans.[10] However, there is little information regarding the interindividual variability of the *in vivo* glucuronosyltransferase activity of 4′-HPPH.

In the present study, to evaluate the interindividual variability of 4′-HPPH glucuronidation, we measured 4′-HPPH and its *O*-glucuronide in urine from patients to whom phenytoin was administered. In addition, the relationship between the interindividual variability and the genetic polymorphisms of UGT1A isoforms in the patients was investigated.

Materials and Methods

Chemicals and regents: 4′-HPPH and β-glucuronidase from *Helix pomatia* (Type H-2) were from Sigma-Aldrich (St. Louis, MO). A Puregene DNA isolation kit was obtained from Gentra Systems (Minneapolis, MN). Taq DNA polymerase was from Greiner Japan (Tokyo, Japan). Restriction enzymes were purchased from Toyobo (Osaka, Japan), Takara (Kyoto, Japan), or New England Biolabs (Beverly, MA). Other chemicals were of the highest grade commercially available.

Patients: This study was approved by the Ethics Committee of Kanazawa University and all the participants gave written informed consent. Fifteen patients (10 males and 5 females) in Kanazawa University Hospital with normal renal and hepatic functions who received phenytoin were studied (**Table 1**). The ages ranged from 18 to 64 years. The daily phenytoin dose varied from 180 to 300 mg. The serum concentration of phenytoin in all patients was expected to be in the steady state, since it has been reported that steady state serum phenytoin levels are achieved 7 to 10 days after phenytoin therapy is begun.[11] The serum concentrations of phenytoin in patients were measured by fluorescence polarization immunoassay (TDX, Dinabot, Tokyo, Japan) as part of a regular monitoring schedule. Urine samples for an entire 24 hr period were collected and frozen at −20°C until analyzed.

Sample preparation: To 0.5 mL urine, 0.5 mL of 0.4 M potassium phosphate buffer (pH 7.4) were added. The mixture was extracted with 4 mL of diethyl ether by shaking for 10 min. The organic fraction was transferred to a clean tube and evaporated under a gentle stream of nitrogen at 40°C. The residue was redissolved in 100 μL of mobile phase and then filtrated with a 0.22 μm filter (Ultrafree®-MC centrifugal filter unit, Millipore, Eschborn, Germany). Aliquots of 5 μL were injected into the LC-MS/MS system. For the determination of glucuronide, urine samples were treated with β-glucuronidase,[12] and measured as 4′-HPPH. To 100 μL urine samples, 800 U/mL of β-glucuronidase were added, and the mixture was incubated at 37°C for 10 hr. After the hydrolysis, the samples were treated as described above.

LC-MS/MS analysis of 4′-HPPH: Liquid chromatography (LC) was performed using an HP 1100 system including a binary pump, an automatic sampler, and a column oven (Agilent Technologies, Waldbronn, Germany), which was equipped with an Inertsil ODS-3 (4.6×250 mm; 5 μm) column (GL Science, Tokyo, Japan). The column temperature was 35°C. The mobile phase was 0.05% formic acid (A) and acetnitrile (B). The conditions for elution was as follows: 30% B (0–18

Table 1. Characteristics of patients in the present study

No	Sex	Age (yr)	Body weight (kg)	Dose of phenytoin (mg/day)	Serum concentration of phenytoin (μg/mL)*	Coadministered drugs	Disease
1	M	53	60	250	NA	—	Meningioma
2	M	26	44	180	8.6	—	Head injury
3	F	48	61	240	6.0	—	Meningioma
4	F	52	49	200	7.6	—	Meningioma
5	M	42	77	300	12.2	Sodium valproate, Thiopental	Status epilepticus
6	M	30	53	200	13.1	Phenobarbital	Hemodialysis access insufficiency
7	M	18	62	200	3.3	—	Cerebral contusion; disturbance of consciousness
8	F	62	63	300	9.4	Betamethasone	Cerebral abscess
9	M	30	69	200	2.5	—	Cerebral aneurysm
10	M	17	53	200	11.6	—	Traumatic subarachnoid hemorrhage
11	F	64	50	200	5.8	Amlodipine, Carvedilol	Meningioma
12	M	44	75	200	3.5	—	Brain tumor
13	M	27	74	200	3.5	—	Brain tumor
14	F	29	44	200	3.7	—	Brain tumor
15	M	18	67	200	3.6	—	Brain tumor

NA: Not available.
*Serum concentration of phenytoin at trough level was measured by fluorescence polarization immunoassay.

min); 30-60% B (18-20 min); 60% B (20-22 min); 60-30% B (22-25 min). Linear gradients were used for all solvent changes. The flow rate was 0.5 mL/min. The LC was connected to a PE Sciex API 2000 Tandem mass spectrometer (Applied Biosystems, Langen, Germany) operated in the negative electrospray ionization mode. Turbo gas was maintained at 500°C. Nitrogen was used as the nebulizing, turbo, and curtain gas at 40, 90, 40 psi, respectively. Parent and/or fragment ions were filtered in the first quadrupole and dissociated in the collision cell using nitrogen as the collision gas. The collision energy was −32 V. Mass/charge (m/z) ion transition was recorded in the multiple reaction monitoring (MRM) mode: m/z 267 and 118. The retention time of 4′-HPPH was 17.0 min. The limit of detection for 4′-HPPH (signal-to-noise ratio 3:1) was 0.4 pmol. The limit of quantification in urine was 2 μM, and it was sufficiently low to quantify 4′-HPPH in urine samples. Linearity was confirmed up to 100 μM and the recovery of 4′-HPPH ranged from 81 to 86%. Intra-day and inter-day precision and accuracy were confirmed to be $<10\%$.

Genotyping: Genomic DNA was extracted from peripheral lymphocytes using a Puregene DNA isolation kit. Genotyping for *CYP2C9*3* (A1075C, Ile359Leu), *CYP2C19*2* (G681A, splicing defect), and *CYP2C19*3* (G636A, stop codon) was performed by PCR-restriction fragment length polymorphism (RFLP) with the restriction enzymes of *Nsi* I, *Sma* I, and *Bam*H I, respectively.[13-15] *UGT1A1*6* (G211A, Gly71Arg), *UGT1A1*7* (T1456G, Tyr486Asp), and *UGT1A1*27* (C686A, Pro229Gln) alleles were genotyped according to a method reported by Ando *et al.*[16] The genotyping methods for *UGT1A1*25* (C840A, stop codon), *UGT1A1*28* (A(TA)$_7$TAA), *UGT1A1*29* (C1099G, Arg367Gly), *UGT1A1*38* (C991T, stop codon), *UGT1A1*60* (T-3263G), *UGT1A1*62* (T247C, Phe83Leu), *UGT1A6*2* (A541G, Thr181Ala and A552C, Arg184Ser), *UGT1A6*3* (A552C, Arg184Ser), *UGT1A9*4* (T726G, stop codon), and *UGT1A9*5* (G766A, Asp256Asn) alleles by PCR-RFLP, PCR-single strand conformation polymorphism (SSCP) or allele-specific (AS)-PCR were developed in the present study (**Table 2**). Genomic DNA samples (0.1 μg) were added to the PCR mixtures (25 μL) consisting of 1X PCR buffer [67 mM Tris-HCl buffer (pH 8.8), 16.6 mM $(NH_4)_2SO_4$, 0.45% Triton X-100, 0.02% gelatin], 1.5 mM $MgCl_2$, 0.4 μM primers, 250 μM dNTPs, and 1 U of Taq DNA polymerase. After an initial denaturation at 94°C for 3 min, the amplification was performed by denaturation at 94°C for 30 sec, annealing for 30 sec, and extension at 72°C for 30 sec for 30 cycles. The final extension step was performed at 72°C for 5 min. Primer sets, restriction enzymes for PCR-RFLP analysis, annealing temperatures, and fragment lengths are summarized in **Table 2**. For PCR-SSCP analyses of the *UGT1A1*28* and *UGT1A1*60* alleles, the PCR products were denatured for 5 min at 80°C with a 5 fold volume of formamide loading dye (96% formamide, 20 mM EDTA (pH 8.0), 0.1% bromophenol blue, and 0.1% xylene cyanol) and loaded onto a 12.5% polyacrylamide gel with 10% glycerol at 25°C and 4°C, respectively. After electrophoresis, the gels were stained with a silver staining kit (Amersham, Buckinghamshire, UK). To confirm the results of the PCR-SSCP analysis, DNA sequencing analysis was performed. The PCR

Table 2. Genotyping method for UGT1A1, UGT1A6, and UGT1A9 polymorphisms by PCR-RFLP, PCR-SSCP or AS-PCR

Polymorphism	Primer set	PCR-RFLP (restriction enzyme), PCR-SSCP (electrophoresis temp.), or AS-PCR	Temperature for annealing	Fragment length	Electrophoresis
			°C	*bp*	
*UGT1A1*6* (G211A, Gly71Arg)	1A1*6S 1A1*6AS	RFLP (*Msp*I)	58	wt: 205, 18 mt: 223	4% agarose
*UGT1A1*7* (T1456G, Tyr486Asp)	1A1*7S 1A1*7AS	RFLP (*Bsr*I)	55	wt: 279,209 mt: 488	2% agarose
*UGT1A1*25* (C840A, stop codon)	1A1*25S 1A1*25AS	RFLP (*Bsa*HI)	58	wt: 165 mt: 145, 20	4% agarose
*UGT1A1*27* (C686A, Pro229Gln)	1A1*6S 1A1*27AS	RFLP (*Bsr*I)	58	wt: 331, 292, 69 mt: 292, 199, 132, 69	2% agarose
*UGT1A1*28* ($A(TA)_7TAA$)	1A1*28S 1A1*28AS	SSCP (25°C)	58	wt: 83 mt: 85	12.5% polyacrylamide
*UGT1A1*29* (C1099G, Arg367Gly)	1A1*29S 1A1*29AS	RFLP (*Msp*I)	57	wt: 826 mt: 528, 298	0.8% agarose
*UGT1A1*38* (C991T, stop codon)	1A1*38S 1A1*38AS	RFLP (*Mnl*I)	55	wt: 214, 86 mt: 300	2% agarose
*UGT1A1*60* (T-3263G)	1A1*60S 1A1*60AS	SSCP (4°C)	56	118	12.5% polyacrylamide
*UGT1A1*62* (T247C, Phe83Leu)	1A1*62S wt or 1A1*62S mt 1A1*6AS	AS-PCR	60	186	2% agarose
*UGT1A6*2* (A541G, Thr181Ala and A552C, Arg184Ser)	1A6S 1A6AS	RFLP (*Nsi*I)	60	wt: 269; mt: 175, 94	2% agarose
*UGT1A6*3* (A552C, Arg184Ser)	1A6*2, *3S 1A6*2, *3AS	RFLP (*Fnu*4HI)	60	wt: 269 mt: 181, 85, 3	2% agarose
*UGT1A9*4* (T726G, stop codon)	1A9*4S 1A9*4AS	RFLP (*Mfl*I)	58	wt: 827 mt: 434, 393	0.8% agarose
*UGT1A9*5* (G766A, Asp256Asn)	first-step: 1A9*4S, 1A9*4AS second-step: 1A9*5S, 1A9*5AS	nested PCR RFLP (*Ava*II)	60	wt: 142, 21 mt: 163	4% agarose

products were subcloned into pT7Blue T-vector (Novagen, Madison, WI). The plasmid DNA was purified by a QIAGEN Plasmid Midi kit (QIAGEN, Valencia, CA) and submitted to DNA sequencing using a thermo sequenase Cy5.5 dye terminator cycle sequencing kit (Amersham Pharmacia Biotech) with a T7F primer (Amersham Pharmacia Biotech). DNA sequences were analyzed on a Long-Read Tower DNA sequencer (Amersham Pharmacia Biotech). The DNA sequences of the primers used for UGT genotyping were as follows:

1A1*6S: 5′-CTC GTT GTA CAT CAG AGC C-3′
1A1*6AS: 5′-GGC CAT GAG CTC CTT GTT GT-3′
1A1*7S: 5′-GAG GAT TGT TCA TAC CAC AGG-3′
1A1*7AS: 5′-GCA CTC TGG GGC TGA TTA AT-3′
1A1*25S: 5′-CCT TGC CTC AGA ATT CCT TC-3′
1A1*25AS: 5′-GAT AGT GGA TTT TGG TGA CG-3′
1A1*27AS: 5′-GTC CCA CTC CAA TAC ACA C-3′
1A1*28S: 5′-ACA CAG TCA AAC ATT AAC TTG-3′
1A1*28AS: 5′-CTA CCA GAG GTT CGC CCT-3′
1A1*29S: 5′-AGA AGC CTT CAC AGT TAC T-3′
1A1*29AS: 5′-CGC TAT TAA ATG CTA CGT AA-3′
1A1*38S: 5′-AGG AAG ATA TCT AAT TCA TA-3′
1A1*38AS: 5′-AGA ATT AAT CTG GAA GCT G-3′
1A1*60S: 5′-GCA CTT GGT AAG CAC GCA A-3′
1A1*60AS: 5′-ATT CTG GAT CCC TTG ATG TT-3′
1A1*62S wt: 5′-AAG ACG TAC CCT GTG CCA T-3′
1A1*62S mt: 5′- AAG ACG TAC CCT GTG CCA C-3′
1A6S: 5′-CAT CAA CTG CCA GAG CCT CC-3′
1A6AS: 5′-GGA AGT TGG CCA CTC GTT GG-3′
1A9*4S: 5′-GGA AAG CAC AAG TAC GGA G-3′
1A9*4AS: 5′-TGG TAC TTT TCT AAA CAT GGT-3′
1A9*5S: 5′-GAA CCA CAT CAT GCA CCT G-3′
1A9*5AS: 5′-GGG ATA GTC CAA AAC AAG